



Corrosion Inhibition of X80 Steel in Simulated Marine Environment with *Marinobacter aquaeolei*

M. Saleem Khan^{1,2} · Dake Xu³ · Dan Liu³ · Yassir Lekbach⁴ · Ke Yang¹ · Chunguang Yang¹

Received: 28 January 2019 / Revised: 11 March 2019 / Published online: 14 May 2019
© The Chinese Society for Metals (CSM) and Springer-Verlag GmbH Germany, part of Springer Nature 2019

Abstract

In the present study, a novel bacterium (*Marinobacter aquaeolei*) was examined for its corrosion inhibiting behaviour against X80 pipeline steel. Electrochemical results showed that X80 steel immersed in the solution inoculated with *M. aquaeolei* possessed very high corrosion resistance compared to that of abiotic control. Besides, scanning electron microscopy, confocal laser scanning microscopy and energy-dispersive X-ray spectroscopy were employed to analyse the corrosion product and the biofilm formed on the metal surface. Fourier-transform infrared spectroscopy was also applied to determine the composition of extracellular polymeric substances (EPS). Above results indicated that the corrosion inhibition efficiency observed in biotic medium was very high (91%), proving that *M. aquaeolei* was an effective inhibitive agent for the corrosion of carbon steel. The inhibition was credited to the formation of bacterial biofilm and the compact protective layer of the secreted EPS. Thus, this study will introduce a natural, environmentally friendly and cost-effective system for the corrosion control of the carbon steel.

Keywords X80 pipeline steel · Corrosion inhibition · *Marinobacter aquaeolei*

1 Introduction

Carbon steel is one of the metallic materials, extensively applied in oil and gas pipelines. However, the lack of some elements like chromium, nickel, and molybdenum makes

this material prone to corrosion, which has always resulted in failures [1, 2]. This structural failure is a big challenge for its application and is responsible for quite a number of losses in different sectors in the form of renovation, modification or change of the applied materials. Moreover, the degrading effects of microbiologically influenced corrosion on the properties of carbon steel have also been reported [3, 4]. Hence, there is a need to extend the service life of the used materials applying corrosion protection techniques [5]. For this purpose, various methods such as surface coating with organic paint, electroplating, biocides and many more corrosion protecting techniques have been used to protect the metals from corrosion [6]. However, these techniques are usually toxic, expensive and non-reliable. Recently, bio-based anti-corrosion agents composed of biological products are the new substitutes for conventional products used for corrosion control [7–9]. The increased interest in the use of natural, environmentally friendly, and cost-effective materials as corrosion inhibitors, the application of bacterial biofilm and their metabolites is getting more attention of the researchers [10].

It has been reported that different factors like biofilm formation which inhibits the oxygen diffusion into the metal surface [11, 12], formation and accumulation of

Available online at <http://link.springer.com/journal/40195>

M. Saleem Khan and Da-Ke Xu have contributed equally to this work.

- ✉ Ke Yang
kyang@imr.ac.cn
- ✉ Chunguang Yang
cgyang@imr.ac.cn

¹ Institute of Metal Research, Chinese Academy of Sciences, Shenyang 110016, China

² University of Chinese Academy of Sciences, Beijing 100049, China

³ Corrosion and Protection Division, Shenyang National Laboratory for Material Sciences, Northeastern University, Shenyang 110819, China

⁴ Laboratory of Microbial Biotechnology, Faculty of Science and Technology, Sidi Mohamed Ben Abdellah University, B.P. 2202, Fez, Morocco

inorganic materials, the biofilm's released antimicrobials, generated bio-surfactants and bacteriophages are contributing to the corrosion inhibition of metals [13–16]. In addition, bacterial EPS also can inhibit the corrosion of the metals [17–19]. This is because EPS contain oxygen, sulphur, and nitrogen in their molecules, which help them to be adsorbed to the metal surface and form a protective layer, thereby shielding the metal from further corrosion [20].

Hence, in the present work, a novel bacterium *M. aquaeolei* was selected to study its corrosion inhibiting behaviour against carbon steel. Electrochemical and surface morphological techniques were performed to investigate the biofilm morphology and the corrosion inhibiting behaviour of this bacteria. The related corrosion inhibiting mechanism was also discussed in depth.

2 Materials and Methods

2.1 Sample Preparation

The used material of X80 pipeline steel with the chemical composition (wt%): 0.028 C; 0.28 Si; 1.90 Mn; 0.008 Nb; 0.22 Mo; 0.20 Cu; 0.08 Cr; 0.29 Ni; 0.03 V; 0.002 S; 0.012 P; and Fe in balance, was provided by Institute of Metal Research, Chinese Academy of Sciences, Shenyang, China. Carbon steel coupons with the dimensions of 10 mm × 10 mm × 5 mm were polished by using silicon carbide paper of different grits from 240 to 1200, followed by rinsing with ethanol and dried in air. All the samples were sanitised under UV light before the experiment.

2.2 Bacterial Cultivation

The investigated bacterium *M. aquaeolei* was purchased from Marine Culture Collection Centre (MCCC) Xiamen, China. The 2216E culture medium prepared by Qingdao Hope Bio-technology Co., Qingdao, China having the following composition (g/L): 19.45 NaCl, 5.98 MgCl₂, 3.24 Na₂SO₄, 1.8 CaCl₂, 0.55 KCl, 0.16 Na₂CO₃, 0.08 KBr, 0.034 SrCl₂, 0.08 SrBr₂, 0.022 H₃BO₃, 0.004 NaSiO₃, 0.0024 NaF, 0.0016 NH₄NO₃, 0.008 NaH₂PO₄, 5.0 peptone, 1.0 yeast extract, and 0.1 ferric citrate was used for the bacterial cultivation. The culture medium (2216E) was sterilized for 20 min at high temperature (121 °C) with the help of an autoclave sterilizer before the experiment. A haemocytometer (light microscope 400× magnification) was applied for measuring the bacterial cells concentration, and the initial cell concentration was 10⁶ cells/mL.

2.3 Electrochemical Experiment

For the electrochemical experiment, a three-electrode glass cell was used having 300 mL of culture medium (2216E) with and without bacterial inoculation. Saturated calomel electrode, platinum electrode and carbon steel sample were the fitted reference, counter, and working electrodes, respectively. Open-circuit potential (OCP), linear polarization resistance (LPR), electrochemical impedance spectroscopy (EIS) and potentiodynamic polarization curves were performed to investigate the microbiologically influenced corrosion (MIC) behaviour of the bacteria. The electrochemical tests were done by using potentiostat (Reference 600™, Gamry Instruments, Inc., USA). LPR measurements were taken at the scan rate of 0.125 mV/s within the potential range of –5 to 5 mV against E_{OCP} . Similarly, the EIS data were obtained using the potential of 5 mV under the frequency range of 0.01–100,000 Hz. Potentiodynamic polarization behaviours were studied at the scan rate of 0.1667 mV/s, and the voltage applied was –0.5 to 0.7 V versus E_{OCP} .

The corrosion inhibiting behaviour of the *M. aquaeolei* EPS was investigated by the immersion of X80 pipeline steel in culture medium with bacterial EPS. The same experimental setup mentioned in Sect. 2.3 was applied here too. OCP, LPR, EIS and potentiodynamic polarization curves of the carbon steel coupons immersed in culture medium with and without bacterial EPS were measured using potentiostat (Reference 600™, Gamry Instruments, Inc., USA). In this study, we used the EPS instead of the bacterial biofilm to investigate its effect on the corrosion resistance of the carbon steel. Electrochemical glass cell having 300 mL medium containing bacterial EPS was used during this experiment.

2.4 Surface Morphology Observation

In order to investigate the bacterial attachment and their activity, the material surface was examined using SEM, CLSM, EDS, XPS and biofilm staining. For all the mentioned techniques, samples immersed in 2216E culture medium with and without bacterial inoculation were incubated at 37 °C for different time. For SEM observation, the coupons were washed with phosphate buffer saline solution and soaked in 4% glutaraldehyde for 4 h to kill and fix the attached bacteria. Afterwards, the samples were dehydrated with an ethanol solution of different concentrations of 50%, 60%, 70%, 80%, 90%, 95%, 100% (V/V) and dried in open air [21]. In order to increase the conductivity, the samples surfaces were coated with gold film and analysed under the scanning electron microscope (Ultra-Plus, Zeiss,

Germany). The EDS analysis was performed to examine the elemental composition of the material surface. For pitting corrosion experiment, the samples were washed in 18% HCl solution containing 20 g/L hexamethylenetetramine to remove the biofilm and corrosion product from the surface [22]. The samples were then inspected under a Zeiss CLSM (LSM 710, Zeiss, Germany).

Live/dead cells staining experiment was performed to examine the bacterial growth and viability on the material surface. The samples were washed with PBS (7.4 pH) and dipped in SYTO-9 and propidium iodide dyes for 20 min in a complete dark environment at room temperature [22]. The used dyes have two colours (green and red), where the green colour represents the live bacterial cells and the red colour represents the dead bacterial cells. A Nikon CLSM (C2 Plus, Nikon, Japan) was applied to observe the biofilm morphology on the material surface. Wavelength of 488 nm was applied for the observation of live cells, while the wavelength applied for the detection of dead cells was 559 nm.

X-ray photoelectron spectroscopy was used to analyse the corrosion product formed on the sample surface. The data were obtained with the aid of XPS (XPS, ESCALAB250 surface analysis system, Thermo VG, USA) using a monochromatic X-ray source (AlK α , line of 1500 eV energy and 150 W power) with binding energy from 0 to 1350 eV. The peak of C1s at 284.6 eV was used to check the charge shifts.

2.5 Fourier-Transform Infrared Spectroscopy (FTIR)

FTIR spectrophotometer (Nicolet Magna-IR 560) with the frequency range of 4000–400 cm⁻¹ and an accuracy of 8 cm⁻¹ was used for the investigation of EPS extracted from the *M. aquaeolei*. The sample (EPS) was mixed with potassium bromide (KBr) and shaped into a thin film which was then observed for its chemical composition.

2.6 Extraction of Extracellular Polymeric Substance (EPS)

Bacteria were cultured in 2216E culture medium for 72 h at 37 °C. Bacterial growth with enough secreted metabolites was observed from the solution colour and viscosity. Then the solution was taken out of the incubator and the bacterial cells were removed with the help of centrifuge followed by filtration using Whatman filter paper with a pore size of 0.22 μm . After filtration, the solution was checked for bacterial contamination by putting 100 μL of the solution on the culture plate containing 2216E culture medium. When no bacterial growth was found on the bacterial plate and no change was observed in the solution colour after 24 h incubation, it was confirmed that there was no bacterial contamination. After successful separation of bacterial cells from the solution, methanol was added into the supernatant for the

precipitation and agglomeration of the polymers. The colour of the supernatant changed to milky white, containing white precipitates of the EPS. Then the solution was centrifuged at 7000 $\times g$ for 5 min at 4 °C, getting EPS to precipitate in the base of tube which was carefully washed using distilled water followed by drying at 30 °C [10]. The extracted EPS was then studied for chemical composition using FTIR.

3 Results and Discussion

3.1 Open-circuit Potential

The open-circuit potential of the X80 pipeline steel is shown in Fig. 1a. The E_{OCP} for the material immersed in bacterial broth and sterile medium showed different trends. The E_{OCP} of the sample in *M. aquaeolei* medium was -676 mV during the first-day experiment and then decreased to a value of -712 mV after 24 h, and remained stable for the rest period of immersion. However, the E_{OCP} of the sample in sterile medium observed at the first day of experiment was -476 mV, which was more positive compared to the sample in bacterial medium. The E_{OCP} for the sterile medium gradually decreased to about -707 mV after 14 days of immersion. The stable E_{OCP} represents that the surface was possibly protected by the biofilm and corrosion inhibitors from corrosion while the negative shift of the E_{OCP} signified the surface dissolution of the material.

3.2 Linear Polarization Resistance (LPR)

In Fig. 1b, the LPR values for the samples in sterile and bacteria inoculated culture medium at the initial immersion days were very low of 11.12 k Ω cm² and 2.14 k Ω cm², respectively. These values were increased with prolonging immersion time and reached to about 13.92 k Ω cm² for abiotic and 163 k Ω cm² for the biotic sample after 7 days. In addition, LPR value of the sample in sterile medium increased to about 32 k Ω cm² after 14 days of immersion, while LPR value of the sample in bacterial solution decreased to about 128 k Ω cm² after 14 days of immersion. The low LPR value in biotic medium was probably due to the bacterial attachment and reaction between the EPS and metallic ions on the surface. This value rapidly increased as the biofilm thickness improved and a protective layer of EPS was formed on the material surface. The decrease of LPR value after 7 days was due to the decrease in the biofilm thickness, caused by the dead bacterial cells in the biofilm. Much bacterial cells were died due to the limited nutrients available in the culture medium, and the biofilm thickness was decreased. Contrarily, the LPR value was very low (32 k Ω cm²) for the abiotic control which showed that the surface was severely aggravated by corrosion-causing elements present in the medium.

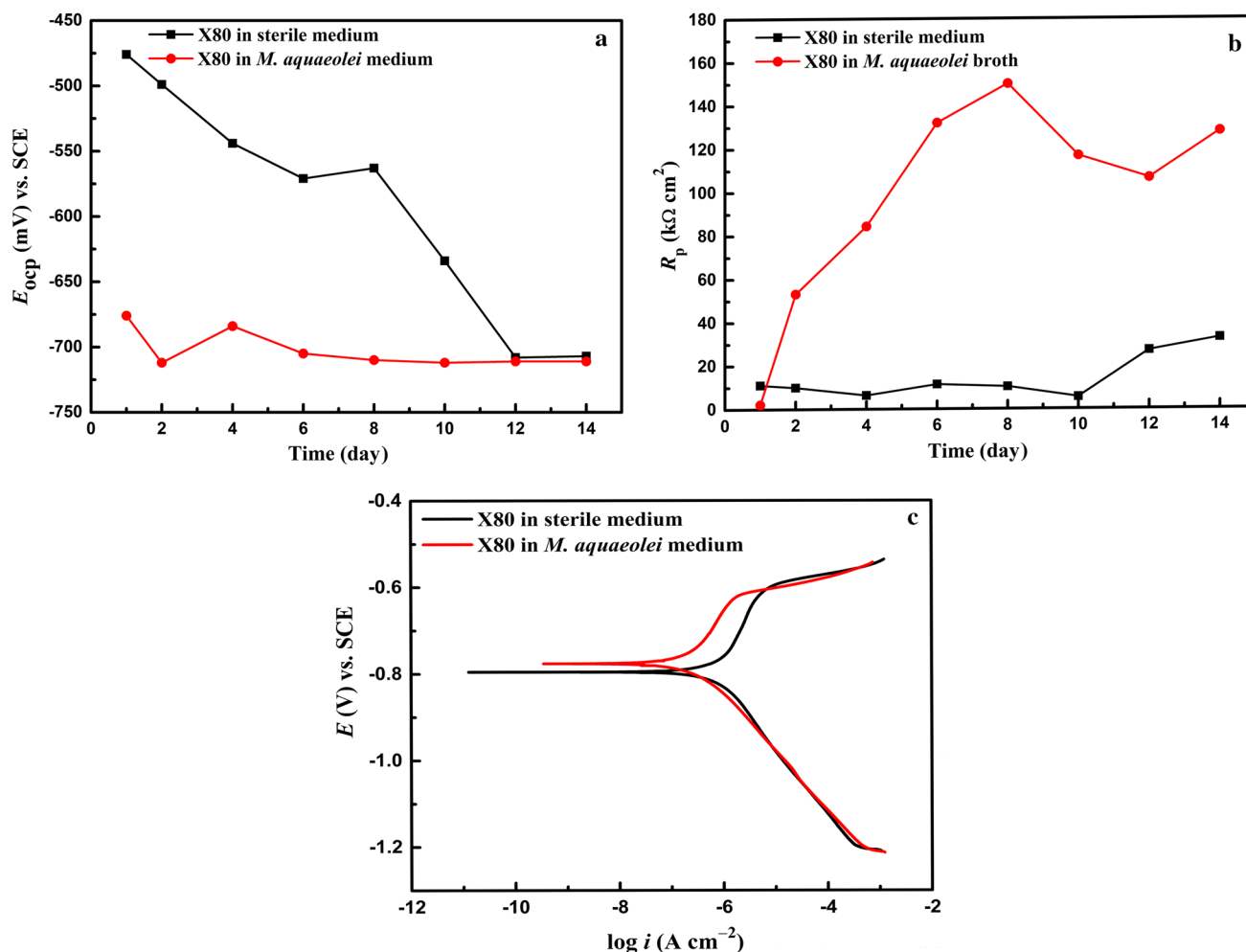


Fig. 1 Open-circuit potential **a**, linear polarization resistance **b**, potentiodynamic polarization curves **c** for the X80 steel in the biotic and abiotic medium

3.3 Potentiodynamic Polarization Behaviour

The polarization curves were derived for the X80 pipeline steel immersed in biotic and abiotic culture medium. Figure 1c shows that the lower corrosion potential (E_{corr}) of -796 mV with higher corrosion current density (i_{corr}) of $1 \mu A cm^{-2}$ in abiotic medium was due to the lower corrosion resistance of the working electrode. The lower corrosion resistance signifies the continuous degradation of this sample during the experiment [23]. While the sample in biotic medium showed E_{corr} of -776 mV and i_{corr} of $0.32 \mu A cm^{-2}$. The lower i_{corr} and higher E_{corr} of the sample in bacterial medium represent its higher corrosion resistance. It was found that the decrease in the corrosion rate in the bacterial medium was due to the mitigation of cathodic and anodic corrosion. Oxygen plays vital role in the process of cathodic corrosion by using the electron releasing during the oxidation of the iron surface that is why the presence of oxygen increases the corrosion rate. Therefore, once the oxygen

contact with the surface of the material is inhibited, the corrosion process can be easily controlled or stopped [24]. In this study, a thick biofilm was formed on the metal surface using the available oxygen for its metabolic activities, which alternatively hindered the cathodic reaction and decreased the cathodic current density [10, 25]. The anodic reaction was also controlled due to the development of EPS layer on the sample surface [26]. The EPS contained compounds with electron-rich functional groups, which were able to make complexes on the surface of the sample and therefore made it passive for further oxidation [27].

3.4 Electrochemical Impedance Spectroscopy (EIS)

EIS is an operative technique for measuring the electrochemical reaction on the corrosion interface. Two electrical equivalent circuits $R_s(Q_{dl}R_{ct})$ and $R_s(C_b(R_b(C_{dl}R_{ct})))$ were built for fitting the EIS data obtained in the sterile and bacterial media. In the electrical circuit, R_s is the solution resistance, Q_{dl}

represents constant phase element due to double layer capacitance, C_b is the capacitance shown by oxide film/biofilm, R_b the combined resistance by oxide film, biofilm, and inhibitors layer, C_{dl} represents the capacitance of the electrical double layer, and R_{ct} symbolizes the charge transfer resistance. The Nyquist and Bode plots are given in Fig. 2. The diameters of the Nyquist plots were larger for the sample immersed in *M. aquaeolei* medium compared to that of abiotic control. Besides, Bode plots for the sample in *M. aquaeolei* inoculated solution showed higher impedance compared to the sample in sterile medium. From EIS data, it is very clear that *M. aquaeolei* offered high corrosion inhibition efficiency to the material. The parameters obtained from the EIS measurements are given in Tables 1 and 2, showing that the R_{ct} for the sample incubated in bacterial medium was increased to 140 $k\Omega\text{ cm}^2$ (7 days) and then decreased to 114 $k\Omega\text{ cm}^2$ after 14 days of immersion. On the other hand, the sample in sterile medium had R_{ct} value of 40 $k\Omega\text{ cm}^2$ after 14 days of incubation. The R_{ct} is inversely proportional to the extent of electrochemical

Table 1 EIS parameters for X80 steel in sterile medium

Immersion time (day)	R_s ($\Omega\text{ cm}^2$)	Q_{CPE} ($\Omega^{-1}\text{ S}^n\text{ cm}^{-2}$)	R_{ct} ($k\Omega\text{ cm}^2$)
1	14.85	1.90×10^{-4}	11.20
4	14.60	7.76×10^{-4}	7.20
7	21.10	7.13×10^{-4}	22.70
14	10.77	1.65×10^{-4}	40.60

reaction [28], implying that a material with high R_{ct} value possesses strong corrosion resistance, and lower R_{ct} represents the low corrosion resistance of the material. The inhibition efficiency measured by using the following equation was 91%, 84% and 65% after 4, 7, and 14 days of immersion in bacterial inoculated medium.

$$\eta_i = \frac{(R_{ct(inh)} - R_{ct(uminh)})}{R_{ct(inh)}} \times 100,$$

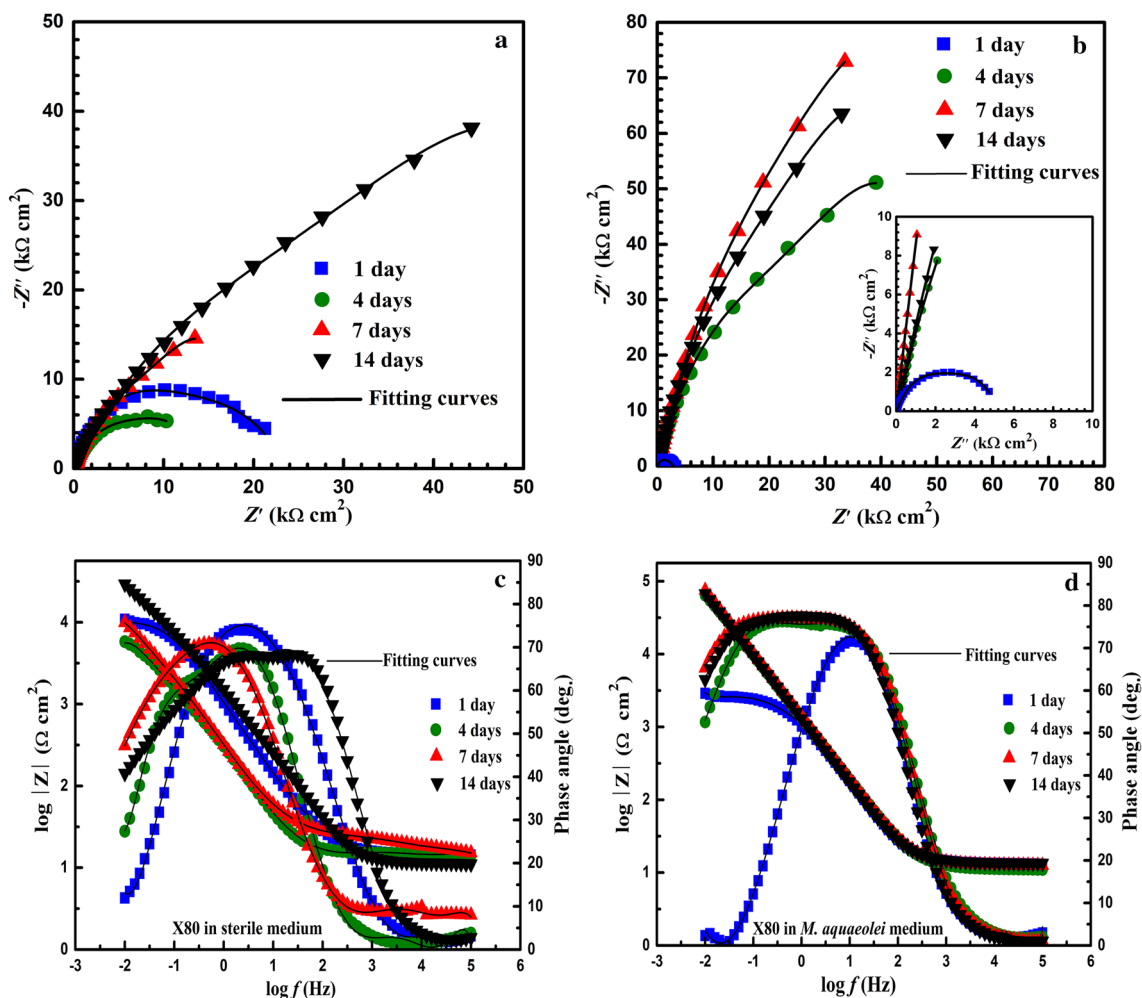


Fig. 2 Nyquist and Bode plots for the material in sterile medium **a, c**, bacteria inoculated medium **b, d**

Table 2 EIS parameters for X80 steel in *M. aquaeolei* broth

Immersion time (day)	R_s (Ω cm ²)	C_b (μ F cm ⁻²)	R_b (k Ω cm ²)	C_{dl} (μ F cm ⁻²)	R_{ct} (k Ω cm ²)
1	14.01	73.64	0.66	98.01	1.80
4	12.12	71.00	1.30	83.70	84.40
7	13.68	72.00	1.88	80.10	140.00
14	14.50	83.00	1.97	85.00	114.00

Here the η_i is the inhibition efficiency, $R_{ct(inh)}$ represents the inhibited while $R_{ct(uninh)}$ represents the uninhibited charge transfer resistance, respectively.

3.5 Scanning Electron Microscopy (SEM)

The sample incubated in bacterial medium was analysed after 7 days of immersion (Fig. 3a), and a uniform biofilm without apparent metal oxide was observed. This represents the attachment of *M. aquaeolei* to the surface, which developed a uniform biofilm and inhibited the surface corrosion. While the sample exposed to the sterile medium showed high number of oxides (Fig. 3b), representing that the material was in contact with the aggressive environment which increased the rate of electrochemical reaction, and thus the surface was corroded. Samples were examined again after 14 days of immersion with SEM for surface morphology

observation, and it showed lesser bacterial cells attachment compared to 7 days of immersion observed in biotic medium (Fig. 3c). Large number of oxides could be seen on the coupon surface incubated in sterile medium (Fig. 3d). In addition, EDS analysis showed high percentage of oxygen and carbon for the sample in bacterial medium compared to the sample in sterile medium, demonstrating the presence of live biofilm on the material surface.

3.6 Confocal Laser Scanning Microscopy (CLSM)

As shown in Fig. 4, the *M. aquaeolei* had very good attachment capacity on the material surface. The bacterium had a very fast growth rate, which can be seen from the biofilm thickness observed after different exposure time. The biofilm thickness measured after 24 h was 31.8 μ m (Fig. 4a), which was increased to 38.3 μ m after increasing the exposure

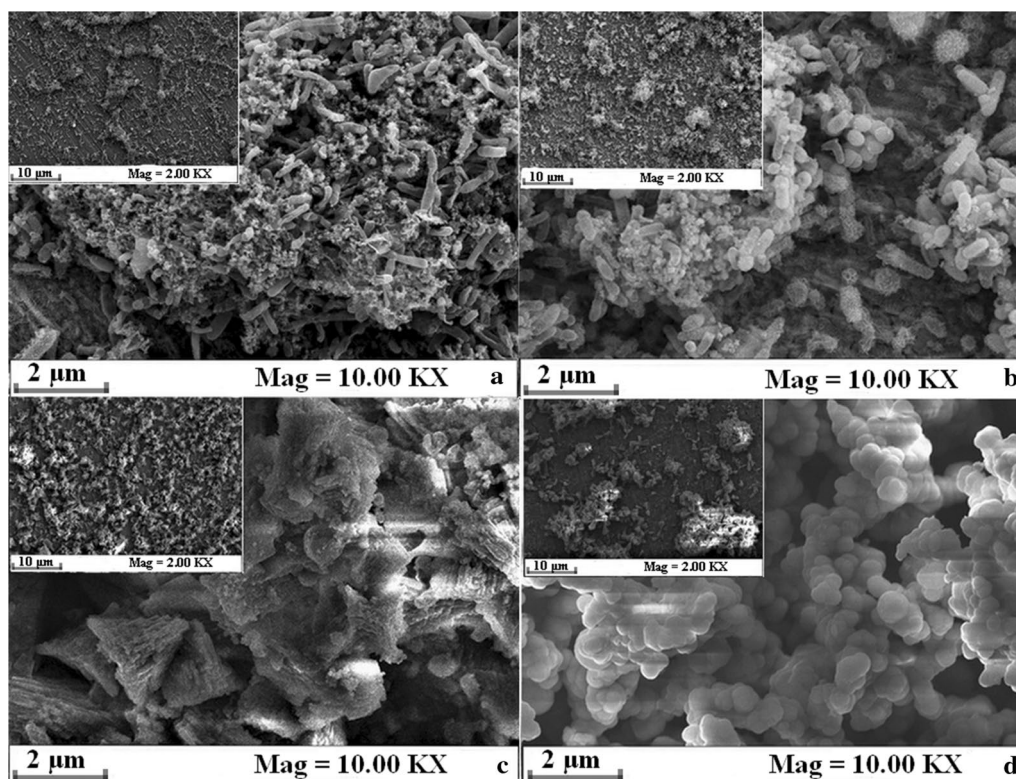


Fig. 3 SEM images of X80 steel immersed in bacteria inoculated medium **a, b** and in sterile medium **c, d** for 7 and 14 days, respectively

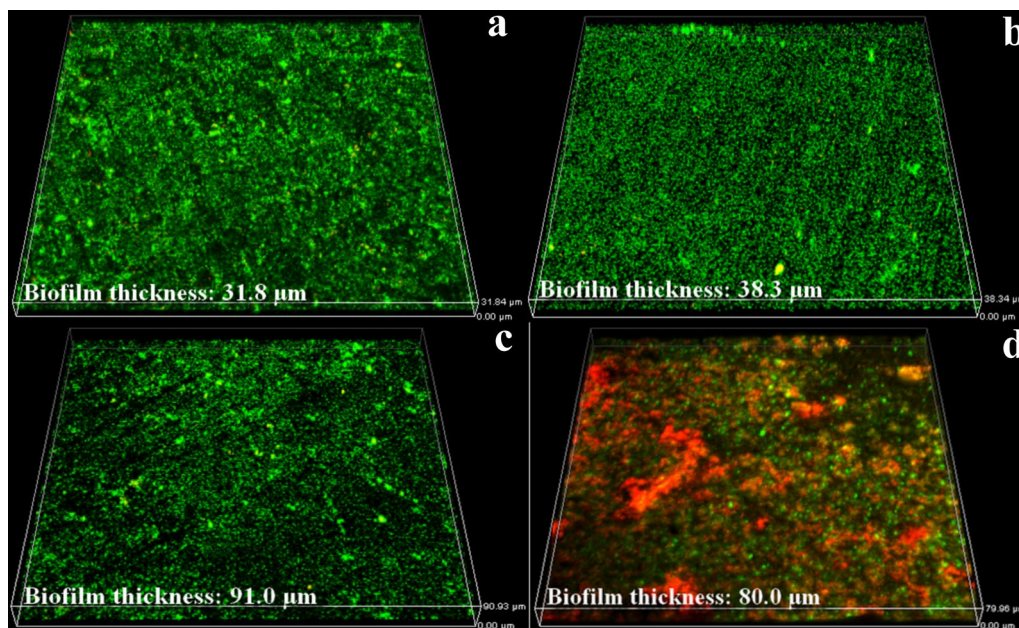


Fig. 4 CLSM live/dead cells test in the *M. aquaeolei* inoculated medium for different exposure time: **a** 24 h, **b** 48 h, **c** 7 days, **d** 14 days

time to 48 h (Fig. 4b). The biofilm thickness was further increased to 91 μm when the sample was exposed to bacterial inoculated medium for 7 days (Fig. 4c). Thereafter, the biofilm thickness decreased to 80 μm by prolonging the exposure time to 14 days. These results are strongly consistent with the electrochemical results. As reported in the electrochemical experiment, the corrosion resistance was increased till 7 days and then decreased, a similar trend was also observed in the CLSM live/dead cells experiment. The biofilm thickness was increased during the first week and then decreased. This means that the biofilm played a key role in the inhibition process, that's why the corrosion resistance was increased with the increase of biofilm thickness and vice versa. The decrease in the biofilm thickness was attributed to the lack of nutrients in the culture medium [29]. Bacterial growth was stopped and enough bacteria were died as no food was available for their nutrition after 14 days of immersion, shown by red colour in Fig. 4d.

The samples were further scrutinized with a confocal laser scanning microscope for pitting corrosion observation. As given in Fig. 5a, the largest pit depth detected after 7 days on the surface in biotic medium was 2.2 μm and the average pit depth found was 0.8 μm . Similarly, the largest pit depth observed on the surface of abiotic control was 5.0 μm and the average pit depth detected was 4.2 μm (Fig. 5b). After 14 days of immersion the sample in bacterial broth had the largest pit depth of 4.6 μm , whereas the average pit depth measured was 4.4 μm (Fig. 5c). Meanwhile, the sterile sample was noticed with largest pit depth of 20.3 μm (Fig. 5d) where the calculated average pit depth was 20.2 μm . The

high resistance to pitting corrosion was due to the formation of biofilm and a protective passive layer of EPS on the material surface. Biofilm used the oxygen which would otherwise be available for the reduction reaction to increase the rate of cathodic corrosion while the EPS layer formed on the surface prevented it from further oxidation. Thus, the inhibition was a synergistic effect of the bacterial biofilm and secreted inhibitors (EPS).

3.7 X-ray Photoelectron Spectroscopy (XPS)

XPS was used for the investigation of corrosion product on the sample surface immersed in biotic and abiotic media, respectively. Figure 6 shows the XPS spectra obtained for X80 steel with and without bacterial inoculation. It can be seen that the biotic sample had four peaks at different binding energies (711.5 eV, 710.3 eV, 722.9 eV and 725 eV), where the peaks with binding energies of 725 eV and 711.5 eV are due to the presence of ferric compounds like iron oxide, iron phosphate and iron-EPS complexes [17]. Besides, the peaks at binding energies of 710.3 eV and 722.9 eV represent the presence of organic ligands, nitrosyl ligands, phenyl/benzyl and carbonyl ligands in complexes with iron (Fig. 6a). While for the abiotic control, the Fe 2p spectra given in Fig. 6b showed four peaks at different binding energies (707.3 eV, 710 eV, 720 eV and 724 eV) corresponding to the metallic iron, Fe_3O_4 , iron in bonding with copper and FeOOH , respectively [30]. The presence of FeOOH and Fe_3O_4 indicates the nature of the corrosion product developed on the surfaces in biotic and abiotic

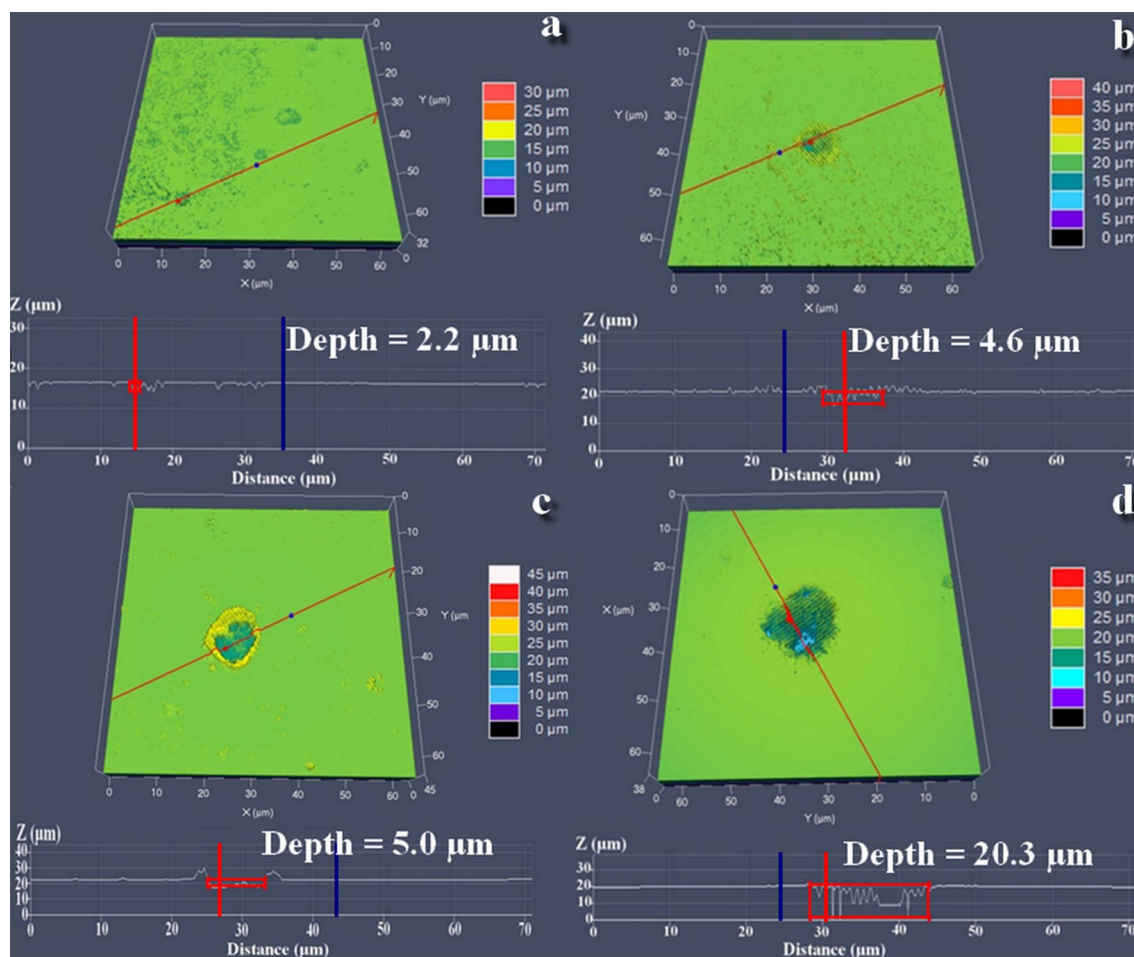


Fig. 5 Pitting corrosion analysis for the samples in biotic medium **a, b** and in sterile medium **c, d** for 7 and 14 days, respectively

media [30–32]. Moreover, the presence of organic compounds demonstrates the attachment of EPS on the surface of the sample immersed in *M. aquaeolei* solution [33].

3.8 Cell-Free Test

As mentioned in the experimental section, the cell-free experiment was performed by using EPS secreted by *M. aquaeolei*. OCP, LPR, EIS and potentiodynamic polarization curves were measured to study the effect of EPS on the corrosion resistance of X80 steel. The electrochemical experiment results are given in Fig. 7. The LPR value for the material exposed to the bacterial EPS was $94 \text{ k}\Omega \text{ cm}^2$ after 14 days of immersion, while the sample in the sterile medium had $65 \text{ k}\Omega \text{ cm}^2$ of LPR value (Fig. 7b). The increase in polarization resistance could be due to the development of a complex structure layer of EPS on the material surface, which protected it from further oxidation. The i_{corr} ($0.426 \mu\text{A cm}^{-2}$) measured for the material incubated with EPS was much lower than the i_{corr} ($0.834 \mu\text{A cm}^{-2}$) of the

sterile sample (Fig. 7c). Two electrical equivalent circuits $R_s(C_fR_{ct})$ and $R_s(C_b(R_b(C_{dl}R_{ct})))$ were used for fitting the EIS data. The charge transfer resistance of the sample immersed in EPS inoculated medium was very high ($90 \text{ k}\Omega \text{ cm}^2$) compared to that of the sterile medium ($68 \text{ k}\Omega \text{ cm}^2$). The R_{ct} increased consistently with increasing the linear polarization resistance. The Nyquist plots represented large diameters in the medium inoculated with bacterial EPS than the sample in a sterile medium. The corrosion inhibition efficiency for the cell-free experiment measured by using the charge transfer resistance was 48%, 51% and 55% after 4, 7 and 14 days of immersion in EPS medium, respectively.

3.9 Fourier-Transform Infrared Spectroscopy (FTIR)

Figure 6c represents the FTIR results of the EPS extracted from *M. aquaeolei*. The FTIR spectrum revealed the existence of polysaccharides, proteins and carbohydrates characteristics. The peak at 3506 cm^{-1} represents the absorbed water molecule [17], while the large adsorption band from

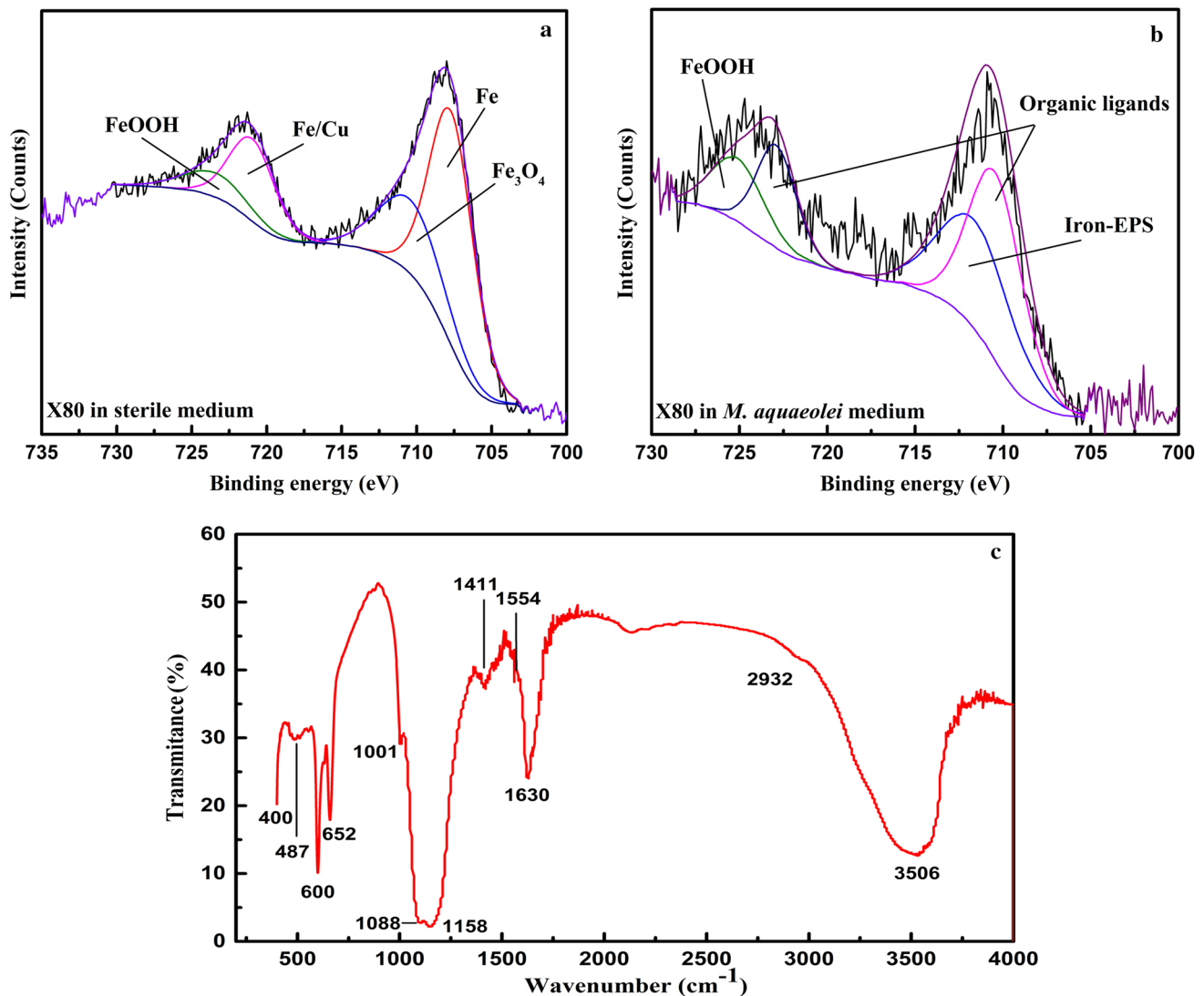


Fig. 6 High-resolution XPS spectra of Fe $2p$ in abiotic medium **a** and biotic medium **b**, FTIR spectrum of the extracellular polymeric substance **c**

3450 to 3506 cm^{-1} was assigned to the polymeric association. The peaks detected at 1630 cm^{-1} and 1411 cm^{-1} were attributed to the asymmetric and symmetric stretching of carboxylates in the side chain [34]. It was noticed that the peak detected at 1630 cm^{-1} is in the lower region, which could be due to the presence of electron donating group in the compound. The peaks at 2932 cm^{-1} and 1554 cm^{-1} were ascribed to the C–H stretching vibration and amide II [35, 36]. Glucosidic bond (C–O–C) was observed as peaks at 1158, 1088 and 1001 cm^{-1} were detected, which notified the presence of pyranyl saccharide in the EPS [35]. FTIR study revealed the presence of proteins, lipids and carbohydrates, which possess plenty of carboxyl and hydroxyl groups. Compounds with carbonyl and amide functional groups were present in a frequent amount in the extracted EPS. Organic compounds with high molecular weight like

proteins and carbohydrates have the ability to adsorb on the metal surface and produce a protective layer [37]. This suggests that the released EPS competed with the bacterial cells for the binding sites available on the surface of the host metal and created a protective layer [38]. The adhering of EPS to the sample surface mitigated the surface dissolution and decreased the anodic reaction.

4 Inhibition Mechanism

The mechanism involved in the process of corrosion inhibition of carbon steel was a synergistic effect of biofilm and secreted EPS (Fig. 8). Inhibition could be the result of the removal of aggressive agents and the formation of a protective layer of EPS on the metal surface [25]. The

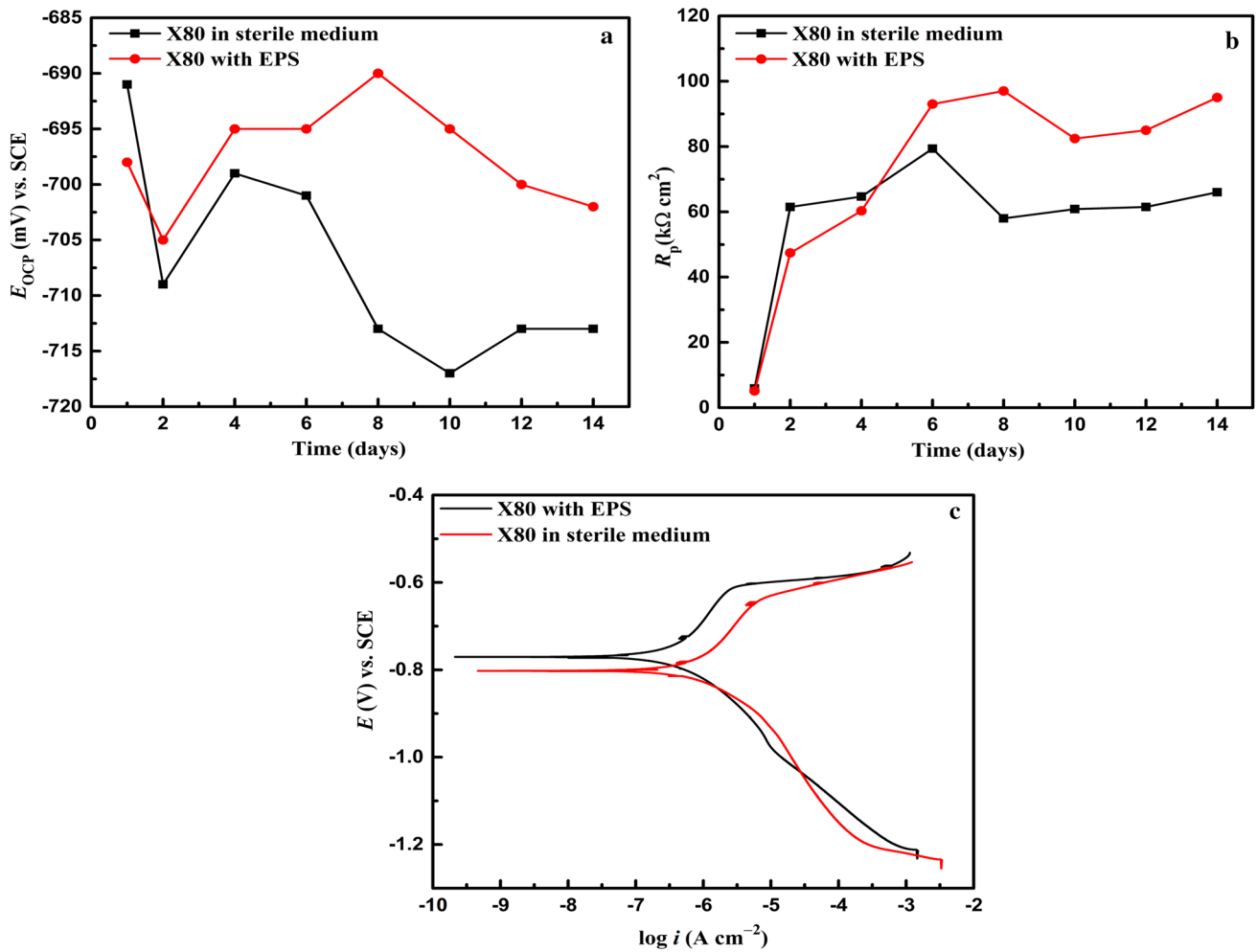


Fig. 7 OCP a, LPR b and potentiodynamic polarization curves c measured for the cell-free experiment

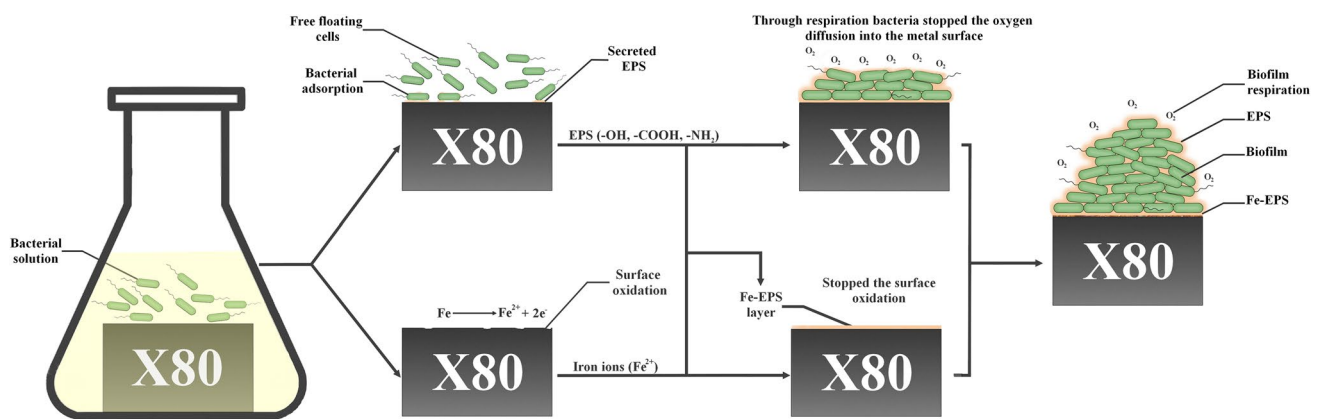


Fig. 8 Mechanistic diagram for the corrosion inhibition of X80 steel by *M. aquaeolei* biofilm and secreted EPS

identification of the passive film formed on the iron surface has been a subject of interest for researchers working in the biocorrosion field [39]. On the basis of above results,

the mechanism of the corrosion inhibition can be drawn. In the beginning, there was no protective layer on the surface, which makes the dissolution of the iron fast and the

corrosion resistance was very weak for the samples with and without bacterial inoculation. As the time passed, the corrosion resistance for the sample immersed in bacteria inoculated culture medium was increased. The increase in the corrosion resistance was indicated by the high value of R_{ct} ($140 \text{ k}\Omega \text{ cm}^2$) measured after 7 days exposure to *M. aquaeolei* medium, which could be due to the bacterial biofilm and the EPS layer formed on the metal surface. On the other hand, a little increase in the R_{ct} value was found for the coupon in sterile medium with prolonging the immersion time, which was attributed to the oxide film formation on the surface [37]. Oxygen which has been considered one of the most corrosive agents for the corrosion of carbon steel was used by biofilm for its physiological activities [25]. It can be seen that the corrosion resistance increased consistently with increasing the biofilm thickness during the first 7 days. The use of oxygen by bacterial cells led to the decrease in cathodic reactions and decreased the corrosion current density [10]. In addition, SEM and CLSM analysis revealed the presence of bacterial biofilm and EPS on the sample surface in biotic medium. EPS contained organic macromolecules such as protein, lipids and carbohydrate, confirmed from the presence of functional groups like hydroxyl, carboxyl and amide in the FTIR analysis. EPS encouraged bacterial cells attachment to the material surface. These macromolecules made a uniform layer on the surface which decreased the corrosion process by preventing the corrosive elements from interacting with the surface [40]. The reactivity of EPS with the metal ions is a well-known phenomenon [17]. EPS makes organometallic complexes by using heteroatoms like oxygen and nitrogen to react with iron ions [38]. Furthermore, it has been reported that EPS can control biocorrosion by bonding with the binding sites at the metal surface which would otherwise be available for the attachment of corrosive bacteria [41]. Through bonding with the metal surface, EPS impedes the active sites and forms a protective layer which shielded the surface from corrosion [42].

Moreover, it was confirmed from the potentiodynamic polarization study that both the anodic and cathodic reactions were controlled which decreased the corrosion rate. Cathodic reaction was mitigated by the oxygen depletion on the surface. Oxygen which acts as an electron acceptor was used by the bacteria for the respiration and was stopped from reaching to the metal surface [27, 43]. Besides, the reaction between EPS and active sites at the metal surface stopped the anodic reactions (iron dissolution) by making a protective layer on the surface and a negative shift in corrosion current density was observed, resulting in decreased corrosion rate [38]. After 14 days of immersion, more dead bacterial cells were found in the biofilm, attributed to the lack of nutrients in culture medium which caused decrease in the biofilm thickness [29]. This decrease in the biofilm thickness caused decrease in the strength of the protective

system provided to the material against corrosion. According to the observations gained during the present work, both biofilm and secreted EPS were found active in the corrosion inhibition of carbon steel.

5 Conclusions

1. X80 pipeline steel possessed high corrosion resistance in biotic medium containing *M. aquaeolei*.
2. The corrosion inhibition was a synergistic effect of the biofilm and secreted EPS. Biofilm performed well in controlling the cathodic corrosion by protecting the carbon steel surface from oxygen contact, while EPS created a uniform layer on the metal surface by complexation with iron ions, which mitigated the surface oxidation of the material.

Acknowledgements Financial support was provided by the Shenzhen Science and Technology Research Funding (Grant No. JCY20160608153641020), the National Natural Science Foundation of China (Grant Nos. 51771199 and 51501188), the National Basic Research Program of China (Grant No. 2016YFB0300205) and the State Key Program of National Natural Science of China (Grant No. 51631009).

References

- [1] Z. Chen, L. Huang, G. Zhang, Y. Qiu, X. Guo, *Corros. Sci.* **65**, 214 (2012)
- [2] K.M. Usher, A.H. Kaksonen, I. Cole, D. Marney, *Int. Biodeterior. Biodegrad.* **93**, 84 (2014)
- [3] D. Xu, Y. Li, T. Gu, *Bioelectrochemistry* **110**, 52 (2016)
- [4] T. Gu, R. Jia, T. Unsal, D. Xu, *J. Mater. Sci. Technol.* **35**, 631 (2019)
- [5] S. Miyajima, Y. Asami, S. Toho, T. Sawada, *Proc. Civ. Eng. Ocean* **22**, 9 (2006)
- [6] R. Jia, T. Unsal, D. Xu, Y. Leckbach, T. Gu, *Int. Biodeterior. Biodegrad.* **137**, 42 (2019)
- [7] F. Tang, X. Wang, X. Xu, L. Li, *Colloids Surf. A Physicochem. Eng. Asp.* **369**, 101 (2010)
- [8] H.T. Dinh, J. Kuever, M. Mußmann, A.W. Hassel, M. Stratmann, F. Widdel, *Nature* **427**, 829 (2004)
- [9] M. Félix, J.E. Martín-Alfonso, A. Romero, A. Guerrero, *J. Food Eng.* **125**, 7 (2014)
- [10] M. Moradi, Z. Song, X. Tao, *Electrochem. Commun.* **51**, 64 (2015)
- [11] H.P. Volkland, G. Repphun, O. Wanner, A.J.B. Zehnder, B. Müller, H. Harms, *Appl. Environ. Microbiol.* **66**, 4389 (2002)
- [12] Y. Li, D. Xu, C. Chen, X. Li, R. Jia, D. Zhang, W. Sand, F. Wang, T. Gu, *J. Mater. Sci. Technol.* **34**, 1713 (2018)
- [13] E. Juzeliunas, R. Ramanauskas, A. Lugauskas, M. Samulevičiene, K. Leinartas, *Electrochem. Commun.* **7**, 305 (2005)
- [14] M. Kingma, *Hum. Resour. Dev. J.* **2**, 1 (1999)
- [15] C. Dagbert, T. Meylheuc, M.N. Bellon-Fontaine, *Electrochim. Acta* **51**, 5221 (2006)
- [16] H.S.C. Eydal, S. Jägevall, M. Hermansson, K. Pedersen, *ISME J.* **3**, 1139 (2009)

- [17] S. Chongdar, G. Gunasekaran, P. Kumar, *Electrochim. Acta* **50**, 4655 (2005)
- [18] H.H.P. Fang, L.C. Xu, K.Y. Chan, *Water Res.* **36**, 4709 (2002)
- [19] I. Majumdar, F. D'Souza, N.B. Bhosle, *J. Ind. Inst. Sci.* **79**, 539 (1999)
- [20] M.A. Malik, M.A. Hashim, F. Nabi, S.A. AL-Thabaiti, Z. Khan, *Int. J. Electrochem. Sci.* **6**, 1927 (2011)
- [21] Y. Lekbach, D. Xu, S. El Abed, Y. Dong, D. Liu, M.S. Khan, S. Ibsouda Koraichi, K. Yang, *Int. Biodeterior. Biodegrad.* **133**, 159 (2018)
- [22] X. Shi, W. Yan, D. Xu, M. Yan, C. Yang, Y. Shan, K. Yang, *J. Mater. Sci. Technol.* **34**, 2480 (2018)
- [23] M. Shepherd, *Br. Med. J.* **2**, 1557 (1979)
- [24] S. Wang, D. Liu, N. Du, Q. Zhao, S. Liu, J. Xiao, *Int. J. Electrochem. Sci.* **10**, 4393 (2014)
- [25] R. Zuo, *Appl. Microbiol. Biotechnol.* **76**, 1245 (2007)
- [26] C. Marins, A. Esteves-souza, C.A. Martinez-huitle, C. José, F. Rodrigues, M. Aparecida, M. Maciel, A. Echevarria, *Corros. Sci.* **67**, 281 (2013)
- [27] A. Jayaraman, E.T. Cheng, J.C. Earthman, T.K. Wood, *J. Ind. Microbiol. Biotechnol.* **18**, 396 (1997)
- [28] Z.H. Dong, T. Liu, H.F. Liu, *Biofouling* **27**, 487 (2011)
- [29] J. Xia, C. Yang, D. Xu, D. Sun, L. Nan, Z. Sun, Q. Li, T. Gu, K. Yang, *Biofouling* **31**, 481 (2015)
- [30] S. Guo, L. Xu, L. Zhang, W. Chang, M. Lu, *Corros. Sci.* **110**, 123 (2016)
- [31] L. Niu, R. Guo, C. Tang, H. Guo, J. Chen, *Surf. Coat. Technol.* **300**, 110 (2016)
- [32] M. Chellouli, D. Chebabe, A. Dermaj, H. Erramli, N. Bettach, N. Hajjaji, M.P. Casaletto, C. Cirrincione, A. Privitera, A. Srhiri, *Electrochim. Acta* **204**, 50 (2016)
- [33] B. Zhang, C. He, C. Wang, P. Sun, F. Li, Y. Lin, *Corros. Sci.* **94**, 6 (2015)
- [34] Q. Bao, D. Zhang, D. Lv, P. Wang, *Corros. Sci.* **65**, 405 (2012)
- [35] J. Qian, W. Chen, W. Zhang, H. Zhang, *Carbohydr. Polym.* **78**, 620 (2009)
- [36] I. Beech, L. Hanjagsit, M. Kalaji, A.L. Neal, V. Zinkevich, *Microbiology* **145**, 1491 (1999)
- [37] C.M. Pradier, P. Bertrand, M.N. Bellon-Fontaine, C. Compère, D. Costa, P. Marcus, C. Poleunis, B. Rondot, M.G. Walls, *Surf. Interface Anal.* **30**, 45 (2000)
- [38] H.J.A. Breur, J.H.W. De Wit, J. Van Turnhout, G.M. Ferrari, *Electrochim. Acta* **47**, 2289 (2002)
- [39] G. Gunasekaran, L.R. Chauhan, *Electrochim. Acta* **49**, 4387 (2004)
- [40] T. Sugama, J.E. DuVall, *Thin Solid Films* **289**, 39 (1996)
- [41] P.J. Antony, R.K. Singh Raman, P. Kumar, R. Raman, *Metall. Mater. Trans. A-Phys. Metall. Mater. Sci.* **39**, 2689 (2008)
- [42] G. Gunasekaran, S. Chongdar, S.N. Gaonkar, P. Kumar, *Corros. Sci.* **46**, 1953 (2004)
- [43] J. Jin, Y. Guan, *Bioresour. Technol.* **169**, 387 (2014)